Range-Dependent Source Localization Methods in Shallow-Water environments

Jing Guo[1, 2], Juan Zeng[1], Li Ma[1]

[1] *Key Laboratory of Underwater Acoustic Environment, Institute of Acoustics, Chinese Academy of Sciences, Beijing 100190, China*

[2] *University of Chinese Academy of Sciences, Beijing 100049, China*

***Abstract* —** In shallow-water environments, the model mismatch due to the spatiotemporal variations in environmental parameters, particularly the sound speed profile (SSP) is a major challenge for matched-field processing (MFP) in passive source localization. In this paper, the sound speed variation in shallow-water environments affected by internal waves is analyzed, and two range-dependent equivalent SSP models, piece-wise linear equivalent model and periodic equivalent SSP model are proposed. These two models are incorporated into the MFP localization algorithm, and both simulation and experimental results, derived from sea trials conducted in the South China Sea, validate their effectiveness. Compared to traditional MFP methods, the algorithm based on the proposed range-dependent equivalent SSP models achieves smaller errors in source range estimation, demonstrating that a range-dependent equivalent SSP model is crucial for improving the source range estimation performance of MFP localization algorithms.

***Key Words* —** source localization, matched-field processing, range dependence, sound speed profile, shallow water

1 Introduction

Passive underwater source localization has been extensively researched for decades, leading to continuous advancements in related techniques. Among the various techniques, matched field processing (MFP) [1] remains a widely used and representative approach. While MFP performs well in stable ocean environments, its effectiveness often degrades in complex and variable ocean conditions. Unlike the large-scale and relatively range-independent deep-sea environment, shallow water is characterized by complex ocean dynamics, resulting in highly variable spatiotemporal sound speed profiles (SSPs). In shallow-water waveguides, range-dependent SSPs and bottom undulations can induce mode coupling among acoustic normal modes [2], which poses challenges for traditional passive localization methods. To address performance degradation caused by environmental model mismatch, numerous adaptive processors for MFP-based localization with improved tolerance to parameter mismatch have been proposed. For example, the Neighborhood Location Constraints method (MV-NLC) [3] enhances robustness to environmental mismatch by introducing constraints to preserve the mainlobe. The Optimal Uncertain Field Processor (OUFP) [4] estimates the source position by maximizing the posterior probability density function of the source location. The Environmental Perturbation Constraints method (MV-EPC) [5] constrains the processor using the statistical characteristics of replica signal covariance matrices computed over a range of perturbed environmental parameters. The Feature Extraction Method (FEM) [6], combined with the Multiple Signal Classification (MUSIC) algorithm, improves robustness by extracting features from the incoherent subspace of the acoustic field.

Despite the advancements, the aforementioned improved MFP algorithms face significant limitations in practical applications. Algorithm-level modifications to the processor do not directly resolve the underlying issue of model mismatch. To address the localization performance degradation caused by environmental parameter uncertainties, Collins and other researchers [7][8] proposed the focalization approach, which jointly estimates both the environmental parameters and the source location.

Among the various ocean environmental parameters, minor errors in seabed geoacoustic properties (such as sound speed, density, and attenuation) typically have limited impact on localization performance. In contrast, mismatch in the water-column SSP can lead to significant degradation in localization accuracy [9]. Therefore, in addition to source range and depth, focalization methods also incorporate the water-column SSP and other unknown or uncertain environmental parameters into the optimization process as variables. A commonly used approach represents the vertical structure of the SSP, as a weighted sum of a background profile and several modes derived from empirical orthogonal functions (EOFs) [10]. This formulation allows for efficient characterization of time-varying SSPs and has thus been adopted in focalization frameworks. Cristiano et al. [11] employed EOFs to construct a range-independent SSP model for joint estimation of the SSP parameters (i.e., EOF coefficients) and source location. For sources at short ranges ($\leqslant$2 km), the EOFs extracted from SSP measurements and the estimated EOF coefficients reflect the temporal variability of the SSP. This approach achieved improved localization performance compared to traditional methods that assume a known SSP. However, as range increases (e.g., 10 km) and source frequency rises, the range dependence of environmental SSP becomes increasingly significant. Consequently, MFP localization methods that consider only temporal variations of the SSP but ignore its range dependence suffer severe performance degradation [12][13].

Accurate passive source localization in shallow-water environments requires effective mitigation of environmental mismatch, particularly due to range-dependent variability in the environmental SSP. The main factor contributing to SSP fluctuations in shallow-water environments is internal wave activity. Internal waves with tidal-cycle characteristics introduce significant spatiotemporal variations in the SSP, which can severely degrade MFP performance. In this study, two range-dependent equivalent SSP models are developed for shallow-water regions of the South China Sea, where internal tides are prevalent. Localization on simulated and experimental data demonstrates the feasibility and effectiveness of range-dependent MFP localization algorithms. The results show that environment-adaptive equivalent SSP models can significantly

enhance localization performance in the presence of internal tidal variability.

2 Sound speed profile models

2.1 Environmental SSP in internal wave environment

In a linear internal wave environment, the motion of seawater particles is typically assumed to be an adiabatic process unaffected by external heat sources. In the two-dimensional (range-depth) domain, the displacement of water particles $\eta(r,z,t)$, can be represented as a superposition of discrete vertical modes [14]

$$\eta(r,z,t) \simeq \sum_{n=1}^{N}\sum_{m=1}^{M} a_{mn}\psi_m e^{i(k_{mn}r-\omega_n t)}\,, \tag{1}$$

where ω_n denotes the frequency of the internal wave, and ψ_m represents the vertical function of the m^{th} mode, characterizing the depth-dependent distribution. Since the vertical modes vary weakly with frequency, they are typically assumed to be independent of ω_n. The horizontal wavenumber of the m^{th} mode at frequency ω_n is denoted by k_{mn}, and a_{mn} is the corresponding modal amplitude, which is determined by the internal wave energy spectrum. The resulting temperature variation due to particle displacement can be approximated as [15]:

$$\frac{\partial T}{\partial t} = -\eta\frac{\partial T}{\partial z}. \tag{2}$$

Integrating Eq. (2) allows the water column temperature profile in a linear internal wave environment to be expressed as a superposition of multiple basis functions [15][16]:

$$T(r,z,t) = T_0(z) + \sum_{m=1}^{M}\sum_{n=1}^{N}\frac{a_{mn}}{i\omega_n}e^{i(k_{mn}-\omega_n t)}\,\varphi_T^m\,, \tag{3}$$

$$\varphi_T^m = \frac{dT_0}{dz}\psi_m\,, \tag{4}$$

where T_0 denotes the background temperature profile, and φ_T^m represents the m^{th} basis function of temperature profile.

In shallow-water environments, the sound speed in the water column exhibits an approximately linear correlation with seawater temperature. Therefore, the SSP can similarly be represented as a combination of a background profile and a superposition of multiple basis functions, and is approximated as:

$$C(r,z,t) \simeq C_0(z) + \sum_{m=1}^{M}\varphi_C^m\sum_{n=1}^{N}A_{(m,\omega_n)}e^{i(k_{mn}r-\omega_n t)}\,, \tag{5}$$

$$\varphi_C^m = \frac{\partial C_0}{\partial z}\psi_m \,, \tag{6}$$

where, $C_0(z)$ denotes the background SSP, φ_C^m is the m^{th} SSP basis function, and $A_{(m,\omega_n)}$ is the corresponding modal amplitude. The horizontal wavenumber k characterizes the spatial variation, while the internal wave frequency ω describes its temporal variability. For different internal wave modes, the nonlinear dispersion relationship between k and ω varies accordingly [14]. In most studies investigating internal wave, the range is often fixed at $r = 0$ to simplify the model—thus focusing solely on the temporal characteristics associated with internal wave frequency. In contrast, if considering the temporal variation of sound speed as a phase modulation superimposed along the spatial domain, then under ideal conditions, the range-dependent SSP in a shallow-water linear internal wave environment can be expressed as:

$$C(r,z) \simeq C_0(z) + \sum_{m=1}^{M} \varphi_C^m \sum_{n=1}^{N} A_{(m,\omega_n)} e^{i(k_{mn} r - \Theta_t^n)} \,, \tag{7}$$

$$\Theta_t^n = -\omega_n t \,. \tag{8}$$

When $t = 0$, the equivalent temporal phase Θ_t^n is zero. In solving inverse problems for focalization methods, an excessive number of model parameters can lead to an exponential increase in computational complexity during multi-parameter optimization. Moreover, model parameter coupling can further degrade the convergence rate of the algorithm. Therefore, constructing an equivalent SSP model with a limited number of parameters that still captures the essential range-dependent characteristics of the environment SSP is critical for the efficiency and effectiveness of range-dependent MFP localization algorithms.

2.2 Range-independent equivalent SSP model

In conventional source localization methods, range-independent equivalent SSPs are commonly constructed using EOFs as basis functions to reduce environmental model mismatch [10]. The range-independent equivalent SSP model can be expressed as:

$$C(z) \simeq C_0(z) + \sum_{m=1}^{M} \varphi_C^m A_m \,, \tag{9}$$

where φ_C^m and A_m denote the m^{th} basis function and corresponding coefficient,

respectively. The background SSP C_0 can be estimated by averaging a set of historical SSP measurements. From the perspective of acoustic field effects, internal wave environments often exhibit strong range-dependent fluctuations in the SSP, which can induce severe coupling between acoustic normal modes [2]. Since range-independent equivalent SSP model cannot capture such features, its effectiveness in mitigating environmental mismatch is substantially limited.

2.3 Range-dependent equivalent SSP model

Conventional MFP algorithms based on range-independent equivalent SSP model primarily focus on capturing the vertical structure and temporal variability of the SSP. By incorporating range-dependent characteristics into these models, it becomes possible to approximate the range dependence of the SSP. As discussed in the analysis of sound speed variability in shallow-water environments, internal waves induce SSP variations with an implicit spatial periodicity. Within a limited range interval, these variations can be approximated as slowly varying linear trends [17]. Therefore, the range-dependent SSP in a linear internal wave environment can be approximated using a piecewise linear model consisting of L segments, and is expressed as:

$$\hat{C} \simeq \left[\widehat{\boldsymbol{C}}_1, \cdots, \widehat{\boldsymbol{C}}_l, \cdots, \widehat{\boldsymbol{C}}_L\right], \tag{10}$$

$$\widehat{\boldsymbol{C}}_l \simeq C_0 + \begin{bmatrix} e_{l,1} & \cdots & e_{l,m} & \cdots & e_{l,M} \end{bmatrix} \begin{bmatrix} \xi_1 \\ \vdots \\ \xi_m \\ \vdots \\ \xi_M \end{bmatrix}. \tag{11}$$

Here, ξ_m denotes the m^{th} order basis function, and $e_{l,m}$ represents its corresponding coefficient in the l^{th} segment. The basis functions ξ_m can be chosen as EOFs extracted from historical SSP data, which contain environmental prior information. Assuming a linear equivalence condition—i.e., the sound speed variation within each segment can be approximated as a slow linear trend—the range-dependent equivalent SSP model described by Eq. (11) can be referred to as a *linear equivalent SSP model*. The linear equivalent SSP model has advantage over conventional range-independent model in describing the complex SSP in shallow water environments.

However, the choice of segmentation interval remains empirical and depends on environmental prior knowledge, due to the discretization introduced by the piecewise segmentation.

Some researchers have employed harmonic analysis methods to study isotherm fluctuations induced by internal tides in shallow water environments. Since isotherms and isospeed lines are closely related, harmonic analysis of isotherms is effectively equivalent to that of sound speed structures. Essentially, the harmonic analysis approach decomposes the SSP into a product of an equivalent mode $\varphi_C^{'}$, which integrates the characteristics of all basis functions, and a series of harmonic components of different orders:

$$C(t,z) \simeq C_0(z) + \varphi_C^{'} \sum_{n=1}^{N} A_n^{'} \, sin(\, \omega_n^{'} t + \Theta_n^{'}) \, . \tag{12}$$

Here, $A_n^{'}$, $\omega_n^{'}$, and $\Theta_n^{'}$ represent the amplitude, frequency, and phase of the n^{th} harmonic component, respectively. Variations in these harmonic components correspond to fluctuations of isospeed contours. The harmonic frequencies ($\omega_n^{'}$) obtained through harmonic analysis are typically associated with the frequencies of internal tidal constituents, and they are related—but not identical—to the internal wave frequencies ω_n. The range dependence of the SSP arises from the combined variations of multiple internal tidal constituents, resulting in a compound spatiotemporal periodicity of the SSP. In certain shallow-water environments dominated by specific tidal constituents—for example, the diurnal tide in the South China Sea [18]—the range dependence of the environmental SSP is primarily governed by that dominant tidal constituent or by the combined influence of several major tidal constituents.

Assuming that the temporal and spatial variations of the sound speed can be approximated as linear changes [19][20], an equivalent tidal constituent can be constructed using only the first-order equivalent vertical function and a set of corresponding coefficients based on the basis function decomposition and harmonic analysis methods. By adding an equivalent compensation, the range-dependent equivalent SSP model with periodic variation characteristics can be expressed as:

$$C(r,z) \simeq C_0(z) + \varphi_C^{'}(A_0^{'} + A_1^{'} \, sin(\frac{2\pi}{T_r^{'}} r + \Theta^{'})) \, , \tag{13}$$

$$T_r^{'} = \frac{2\pi}{\omega^{'}}, \tag{14}$$

where, $\varphi_C^{'}$ denotes the equivalent basis function, and $A_0^{'}$, $A^{'}$, $\omega^{'}$, and $\Theta^{'}$ represent the compensated bias, amplitude, frequency, and phase of the equivalent tidal constituent, respectively. $T_r^{'}$ is the wavelength of the equivalent tidal constituent, corresponding to the horizontal periodicity of the SSP. The range-dependent equivalent SSP model based on the equivalent tidal constituent, as expressed in Equation (13), is hereafter referred to as the *periodic equivalent SSP model*. Compared to the linear equivalent SSP model, the periodic equivalent SSP model provides a more continuous and effective representation of the spatial periodicity of the environmental SSP, particularly in regions dominated by internal tidal waves. However, the modeling approach based on the equivalent tidal constituent also limits the applicability.

3 Range-dependent MFP algorithm

In this section, the impact of different equivalent SSP models on the performance of MFP-based source localization will be investigated through numerical simulations. Simulations are performed under shallow-water conditions representative of the South China Sea, following the experimental setup. The widely used *Bartlett* processor is employed to localize simulated acoustic sources,

$$F(\alpha, \beta, r, z) = \frac{1}{N_f} \sum_{j=1}^{N_f} \left| V_{r,z}{}^{H} \boldsymbol{X} \right|^2 . \tag{15}$$

Signal composed of multiple frequency points is emitted from a source located at a depth r and a range z. N_f denotes the number of frequency points to be calculated, $\boldsymbol{X}$ represents the observed acoustic field vector measured by the receiving array, and $V_{r,z}$ is the computed replica field. α represents parameters related to SSP and β represents other environmental parameters. The normalized two-dimensional ambiguity surface over distance and depth is defined as follows:

$$Surface(r, z) = 10\, log_{10}\left(\frac{F(\alpha_{opt}, \beta_{opt}, r, z)}{max\{F(\alpha_{opt}, \beta_{opt}, r, z)\}}\right) . \tag{16}$$

Acoustic fields are computed using the range-dependent acoustic model (RAM), and genetic algorithm (GA) is employed as the optimization method, with the acoustic field

correlation $F(\alpha, \beta, r, z)$ serving as the objective function. The GA parameters are set as follows: generation gap of 0.9, crossover probability of 0.9, and mutation probability of 0.05. Multi-parameter optimization is performed via multiple parallel searches, with a population size of 40 individuals evolving over 50 generations, resulting in a total of 2000 parameter vectors evaluated.

In the summer of 2020, the Institute of Acoustics, Chinese Academy of Sciences, conducted a fixed-point acoustic fluctuation experiment in the South China Sea. Figure 1(a) presents the measured 30-hour SSP measurements ensemble from the experiment. The internal wave activity during the experiment is dominated by the diurnal tide (24 h). A segment of the SSP measurements is transformed into a range-dependent SSP using an internal wave propagation speed of 1 m/s [18], representing the simulation environment of the South China Sea, as illustrated in Fig. 1(c). The first three EOFs extracted from the SSP measurements are shown in Fig. 1(b). The first EOF accounts for approximately 78% of the variance, thus serving as the basis function in both the linear equivalent SSP model and the periodic equivalent SSP model sufficiently characterizes the vertical structure of SSP. The range-independent equivalent SSP model uses all the first three EOFs.

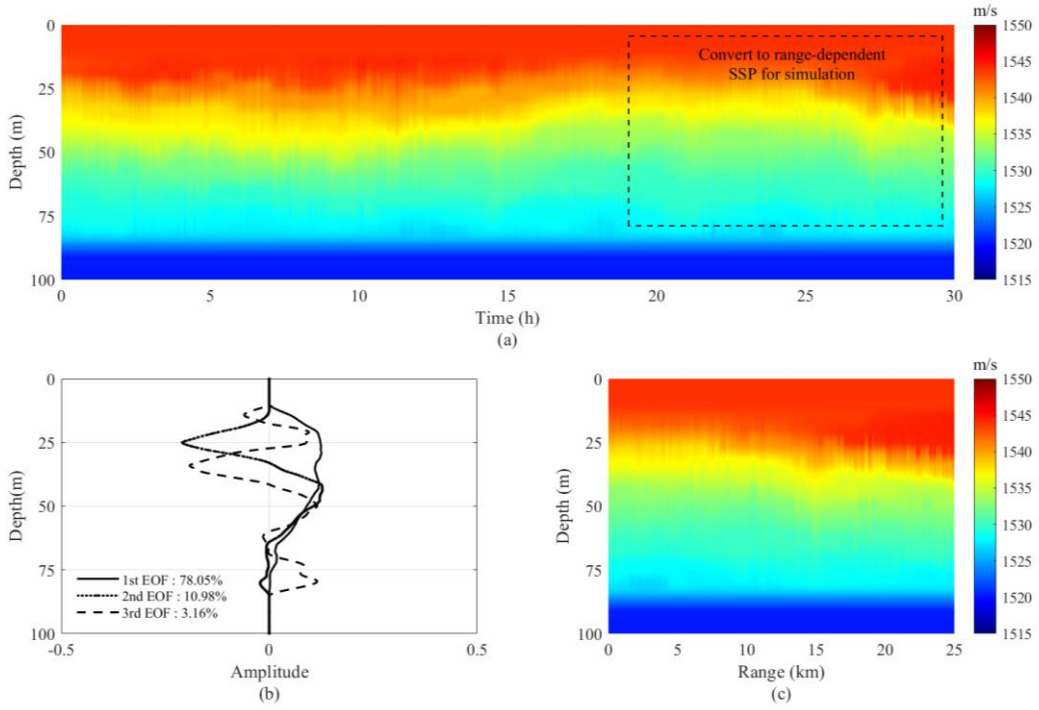

Fig. 1. Sound speed profile information from the South China Sea.

(a) 30-hour SSP measurements; (b) First three EOFs; (c) 25-km simulated SSP.

It is noteworthy that the dominant tidal constituent in the shallow waters of the South China Sea is the diurnal tide, which has a relatively long wavelength (approximately 77–86 km [18]). Since the 20-km SSP along the acoustic propagation path accounts for only about one-third of the diurnal tide wavelength, higher-frequency tidal constituents tend to dominate the sound speed variability over such shorter ranges. Therefore, the search range for the equivalent tidal wavelength (T') in the periodic equivalent SSP model should be adjusted accordingly. For example, in the South China Sea experimental environment, the semidiurnal tide—aside from the dominant diurnal tide—has the second-largest energy contribution, with a wavelength of approximately 40 km [18]. Accordingly, the wavelength T' of the equivalent tidal constituent is constrained to a search range of 20–60 km. In the case of the linear equivalent SSP model, a segment interval of $\Delta r = 4$ km is selected, resulting in six linear-equivalent profiles and a total of seven model parameters. Table 1 lists other relevant parameters, including seabed properties, vertical line array (VLA) configuration, and source information. The maximum acoustic propagation range is set to 24 km, with a range step size of 10 m. Table 2 summarizes the parameter search ranges and estimation results for each algorithm under the South China Sea simulation scenario.

Tab. 1. Simulation environment parameter settings.

Seabed			Vertical line array			Source		
sound speed	density	attenuation	element count	element spacing	depth coverage	range	depth	signal frequency
m/s	g/cm3	dB/λ	\	m	m	km	m	Hz
1650	1.75	0.2	16	1.5	32.5~55	20	55	320 340 360 380 400

Tab. 2. Parameter search ranges and localization results in the South China Sea simulation.

Source localization algorithms	Parameter search range of equivalent SSP model							Source location	
	A_1	A_2	A_3	A_0'	A_1'	T_r' (km)	Θ'	depth (m)	range (km)
	[-15,15]	[-10,10]	[-5,5]	[-10,10]	[5,15]	[20,60]	$(-\pi, \pi]$	[20,80]	[16,24]
Range-independent MFP	-10.11	-3.54	-4.93	\	\	\	\	41	16.4
Periodic MFP	\	\	\	-0.38	13.93	25.46	-0.12 π	48	19.4
\	e_1	e_2	e_3	e_4	e_5	e_6	e_7	depth (m)	range (km)
	[-25,25]	[-25,25]	[-25,25]	[-25,25]	[-25,25]	[-25,25]	[-25,25]	[20,80]	[16,24]
Linear MFP ($\Delta r = 4$ km)	8.43	12.72	-24.16	-18.97	-14.35	12.21	3.31	56	19.6
Linear MFP ($\Delta r = 6$ km)	8.08	-19.87	-19.21	14.17	24.89	\	\	55	19.6

Figures 2 and 3 show the localization ambiguity surfaces and reconstructed equivalent SSPs obtained by different algorithms. The actual source location and the estimated position are marked with symbols “O” and “X” on the ambiguity surfaces, respectively. The range-independent MFP algorithm [Fig. 2 (d)], which does not account for the range-dependence of SSP, fails to locate the source, resulting in large localization error. The two range-dependent equivalent SSP models introduce horizontal variability, which helps mitigate the mismatch between the assumed and environmental SSPs, thereby enhancing localization performance. Compared to the range-independent MFP algorithm, which yields a source range estimate of 16.4 km, the linear MFP algorithm ($\Delta r = 4$km) and the periodic MFP algorithm provide more accurate estimates of 19.6 km and 19.4 km, respectively, closer to the actual source range of 20 km. By incorporating range-dependent features in the SSP, the localization error is significantly reduced from 3600 m to 400 m. The equivalent SSPs reconstructed by the range-dependent algorithms capture main features of the environmental SSP variations and better account for mode coupling effects, resulting in improved localization accuracy over the range-independent MFP algorithm.

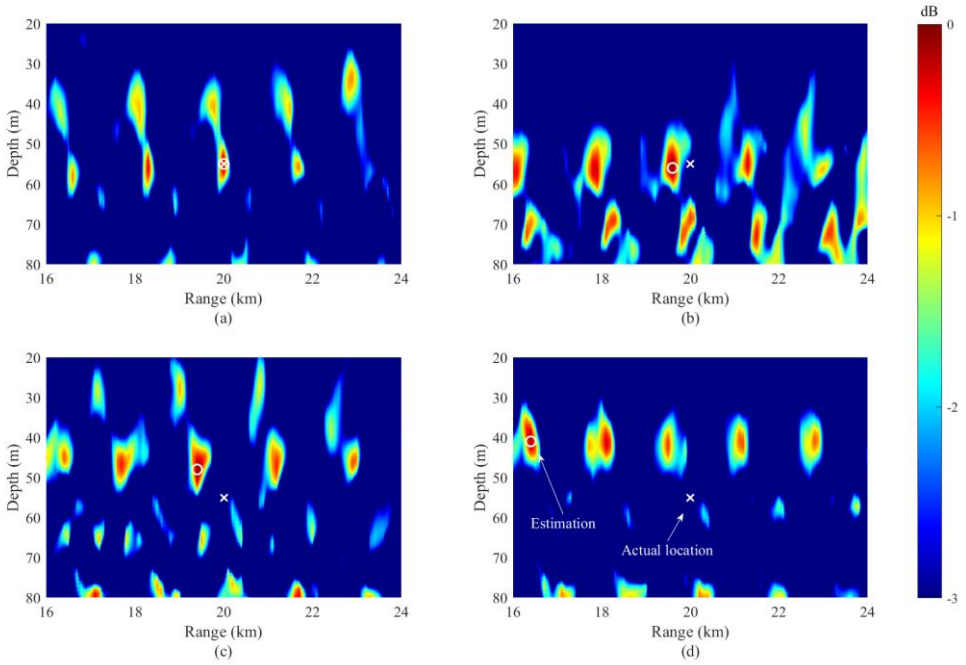

Fig. 2. Localization ambiguity surfaces for different algorithms in simulation.

(a) MFP without mismatch; (b) Linear MFP;

(c) Periodic MFP; (d) Range-independent MFP.

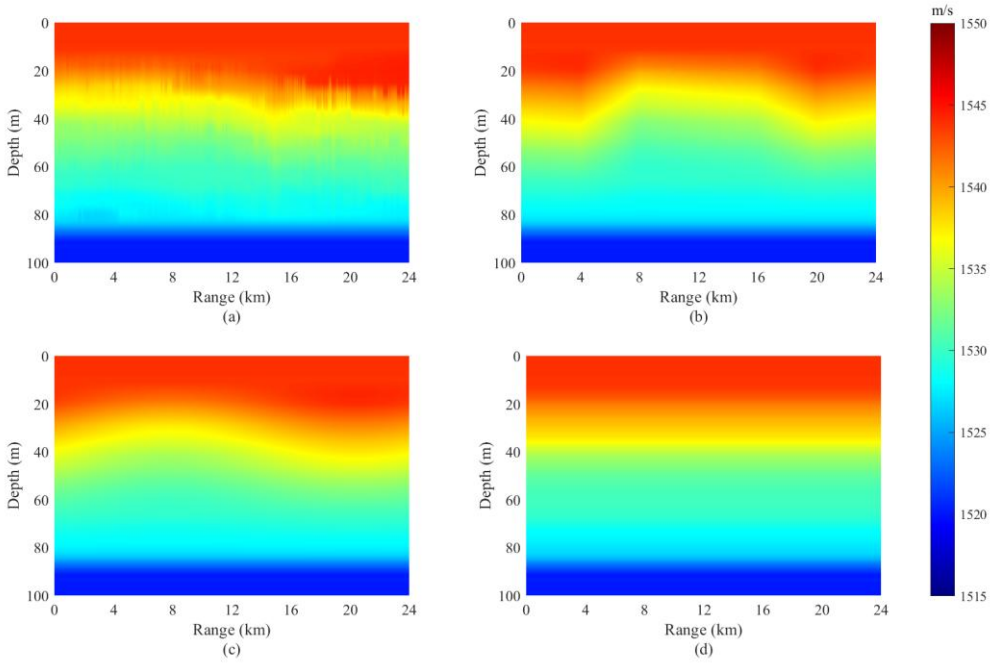

Fig. 3. Reconstructed equivalent sound speed profiles in simulation.

(a) SSP of the simulation environment; (b) Linear equivalent SSP;

(c) Periodic equivalent SSP; (d) Range-independent SSP.

The continuously varying periodic SSP model incorporates certain physical features (e.g., tidal periodicity), and its closer alignment with environmental characteristics enables improved localization performance [Fig. 3(c)]. In contrast, the linear equivalent SSP model produces discrete SSP segments [Fig. 3(b)], and strongly depends on the chosen segment interval. The reconstructed equivalent SSPs from the two range-dependent MFP localization algorithms reflect the general trend of environmental variability in simulation, but discrepancies remain when compared to the SSP of the simulation environment, especially for the linear equivalent SSP with a segment interval of $\Delta r = 4$ km. To further investigate the effect of segmentation choice, linear MFP algorithm is performed with a larger segment interval of $\Delta r = 6$ km (i.e., four segments), which better matches the trend of SSP variation in the simulation environment. Figure 4 presents the localization ambiguity surface and the reconstructed equivalent SSP for the linear MFP algorithm with $\Delta r = 6$ km. The corresponding parameter search ranges and localization results are listed in Table 2.

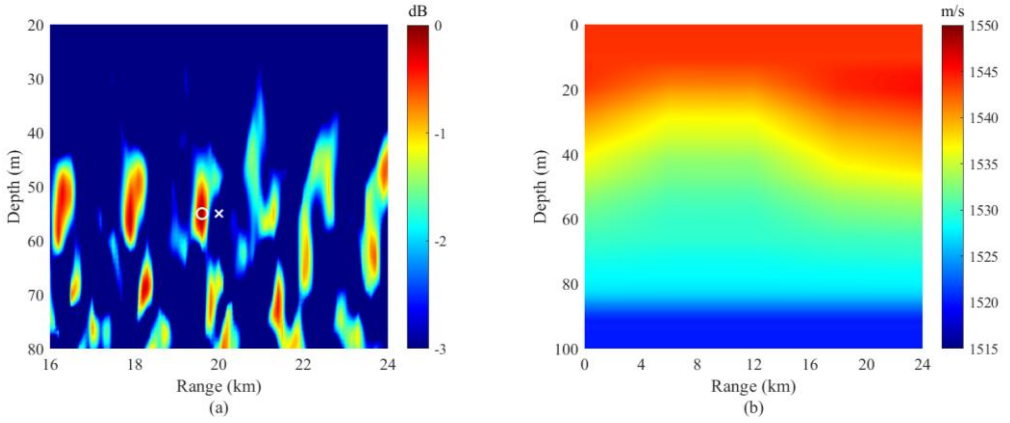

Fig. 4. Results of the linear MFP algorithm with segment interval $\Delta r = 6$ km.

(a) Localization ambiguity surface; (b) Reconstructed equivalent SSP.

While the four-segment linear MFP successfully localized the source, its ambiguity surface [Fig. 4(a)] exhibits more dispersed sidelobe patterns compared to the six-segment result with $\Delta r = 4$ km [Fig. 2(b)]. This suggests that denser segmentation can provide stronger fitting capability. However, due to the discrete nature of the segmentation approach, the equivalent SSP reconstructed with the more suitable interval ($\Delta r = 6$ km) offers a better match to the overall trend of the environmental

SSP [Fig. 4(b)]. Furthermore, figure 5 shows a comparison of the first-order EOF coefficient curves reconstructed by different algorithms, indicating that both the linear MFP ($\Delta r = 6$ km) and the periodic MFP provide estimates more consistent with the environmental EOF curve in simulation.

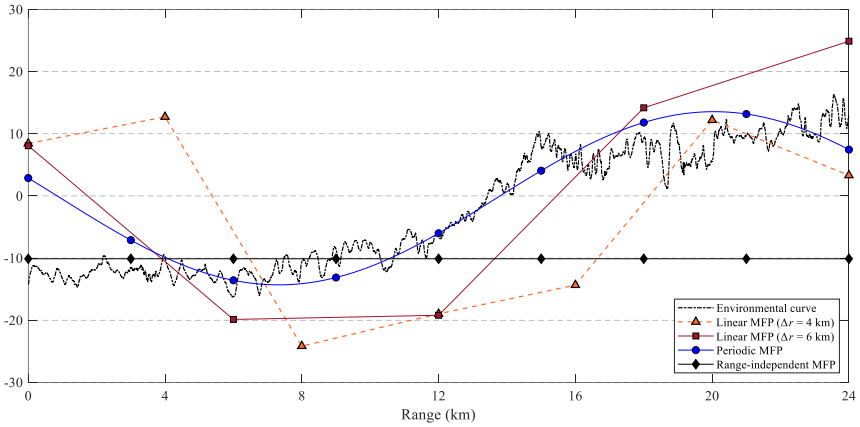

Fig. 5. First-order EOF coefficient curves reconstructed by different algorithms.

Although the range-dependent equivalent SSP models can characterize range dependence of the environmental SSP, the primary goal of the range-dependent MFP localization algorithm is not to invert the actual environmental SSP. Instead, the algorithm aims to optimize the model parameters to maximize the field matching function $F(\alpha, \beta, r, z)$. Under the given model assumptions, the algorithm searches within the model parameter space to find the set that maximizes the objective function. Whether the reconstructed equivalent SSP accurately represents the environmental SSP depends heavily on the accuracy of environmental modeling and the availability of sufficient prior information to solve the nonlinear multi-parameter optimization problem, and both of which are difficult to achieve in real-world environments. In summary, the localization results in the South China Sea simulation environments demonstrate that, in shallow-water environment with internal waves, the range-dependent MFP algorithms based on the linear and periodic equivalent SSP models achieve better localization performance than the commonly used range-independent MFP algorithm.

4 Experiment Validation

As a supplement to the previously described experiment in the South China Sea, the deployment of the experimental equipment is illustrated in Fig. 6. The acoustic source was a low-frequency transducer suspended 55 m below the vessel, transmitting linear frequency modulated (LFM) signals with a frequency range of 320–400 Hz, a duration of 10 seconds, and a repetition interval of 45 seconds. A vertical line array consisting of 16 hydrophones spaced 1.5 m apart was deployed approximately 20 km from the source to serve as the receiver. During the experiment, the hydrophone depths exhibited periodic fluctuations due to large-scale internal wave activity. The uppermost hydrophone was located at a depth of 32.5 m, and the bottom hydrophone at 55 m, with both remaining relatively stable at these depths during the stable period. Due to experimental constraints, the array was deployed in shallow water and spanned only about one-quarter of the total water depth. Source localization is conducted using three algorithms while the array remained in a stable configuration: a range-independent MFP algorithm and two range-dependent MFP algorithms based on the linear and periodic equivalent SSP models, respectively.

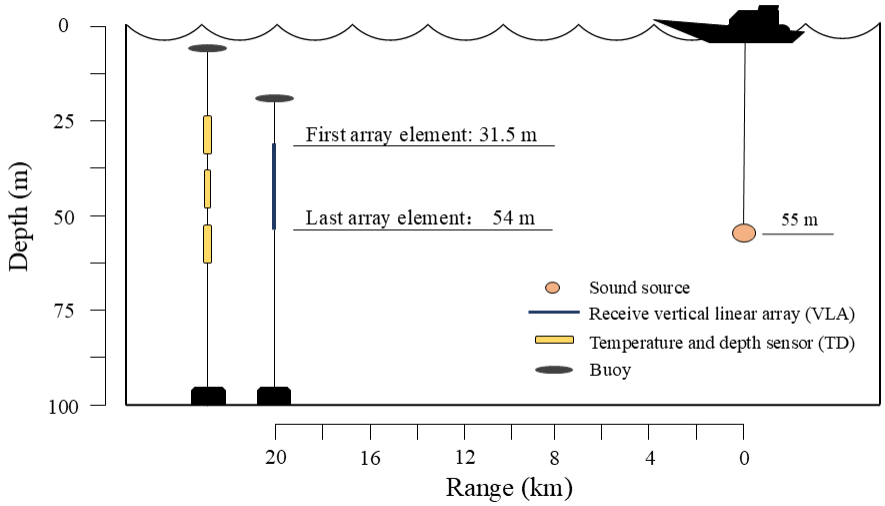

Fig. 6. The equipment deployment of the experiment in the South China Sea.

In the numerical simulation, seabed parameters are assumed to be known. However, in real environments, these parameters—such as seabed sound speed, density,

and attenuation—are typically unknown and should be jointly estimated along with the SSP, source depth, and source range. To solve this nonlinear multi-parameter optimization problem, genetic algorithm (GA) with multiple parallel search groups was employed. The GA parameters are set with a generation gap of 0.9, a crossover probability of 0.9, and a mutation probability of 0.05. A total of 10,000 parameter vectors are evaluated during the optimization process. The segmentation intervals for the linear equivalent SSP models are set to $\Delta r = 4$ km and $\Delta r = 6$ km, consistent with the numerical simulation and satisfying the conditions for linear approximation. The equivalent tidal wavelength $T_r^{'}$ for the periodic equivalent SSP model is selected based on the tidal constituents observed in the environment, consistent with the search range used in the numerical simulations. All the parameter search ranges and the localization results for a representative experimental signal are summarized in Table 3.

Tab. 3. Parameter search ranges and localization results in the South China Sea experiment.

			Range-independent MFP	Periodic MFP			Linear MFP ($\Delta r = 4$ km)	Linear MFP ($\Delta r = 6$ km)
Equivalent SSP Model parameters	A_1	[-15,15]	13.94	\	e_1	[-25,25]	8.69	6.93
	A_2	[-10,10]	-3.92	\	e_2	[-25,25]	17.49	14.24
	A_3	[-5,5]	3.09	\	e_3	[-25,25]	-11.97	-7.09
	A_0'	[-10,10]	\	7.74	e_4	[-25,25]	-15.19	-16.97
	A_1'	[5,15]	\	6.71	e_5	[-25,25]	19.88	10.02
	T_r' (km)	[20,60]	\	34.07	e_6	[-25,25]	14.58	\
	Θ''	$(-\pi, \pi]$	\	0.86 π	e_7	[-25,25]	1.27	\
Seabed parameters	sound speed (m/s)	[1550,1650]	1586	1559			1554	1597
	density (g/cm3)	[1,2]	1.74	1.48			1.39	1.58
	attenuation (dB/λ)	[0,1]	0.29	0.81			0.91	0.75
Source location	depth (m)	[20,80]	59	57			51	59
	range (km)	[16,24]	18.8	19.4			20.2	20.7

The equivalent SSPs reconstructed by the range-dependent and range-independent MFP algorithms, along with the estimated localization ambiguity surfaces, are shown in Fig. 7. The algorithmic estimates and the actual source position are marked by "O" and "X" on the ambiguity surfaces, respectively. The range-dependent MFP algorithms based on the linear and periodic equivalent SSP models account for the range dependence of the environmental SSP. Compared to the 1200 m range estimation error of the range-independent MFP, the range estimation errors are reduced to 200 m, 700 m, and 600 m for the linear MFP with $\Delta r = 4$ km, linear MFP with $\Delta r = 6$ km, and periodic MFP, respectively. The introduction of range-dependent equivalent SSP models significantly improved the range estimation performance of the MFP algorithms. Both the linear and periodic MFP algorithms effectively approximate the mode coupling effects induced by internal waves. Figure 8 presents the equivalent SSPs reconstructed by the four localization algorithms.

Notably, the equivalent SSPs reconstructed by the linear MFP with $\Delta r = 6$ km and the periodic MFP exhibit similar trends along the range [Fig. 8(b) (c)], and their range estimation errors are comparable. However, during the optimization process—where the objective function is the field matching function $F(\alpha, \beta, r, z)$—the linear MFP with $\Delta r = 4$ km benefits from a greater number of model parameters, resulting in a smaller range estimation error of 200 m. Overall, the processing of experimental data confirms the necessity of considering the range dependence of environmental SSP. Establishing an appropriate range-dependent equivalent SSP model can enhance the localization performance of MFP algorithms in shallow-water internal wave environments.

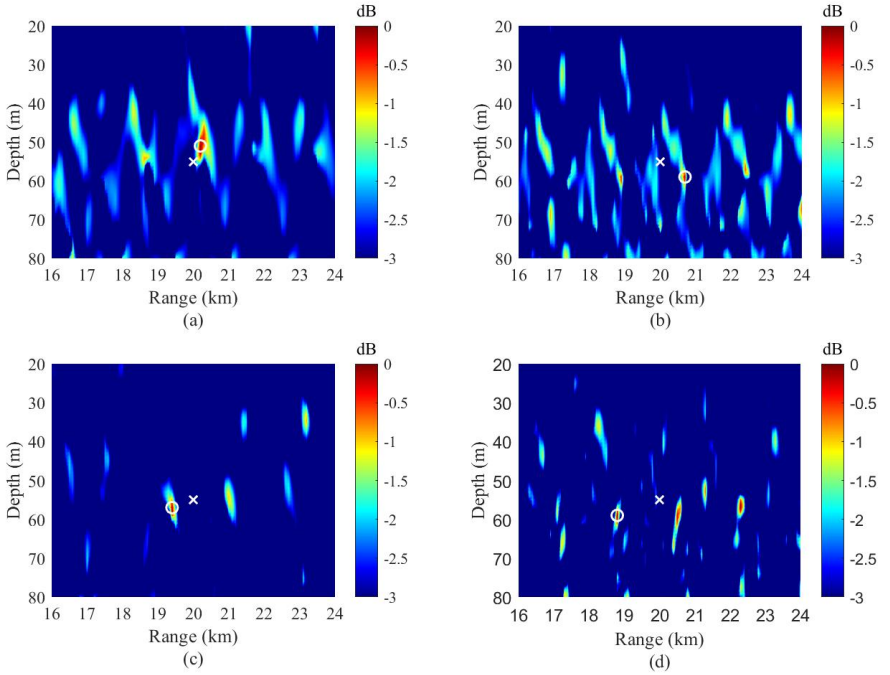

Fig. 7. Localization ambiguity surfaces for different algorithms in experiment. (a) Linear MFP ($\Delta r = 4$ km); (b) Linear MFP ($\Delta r = 6$ km); (c) Periodic MFP; (d) Range-independent MFP.

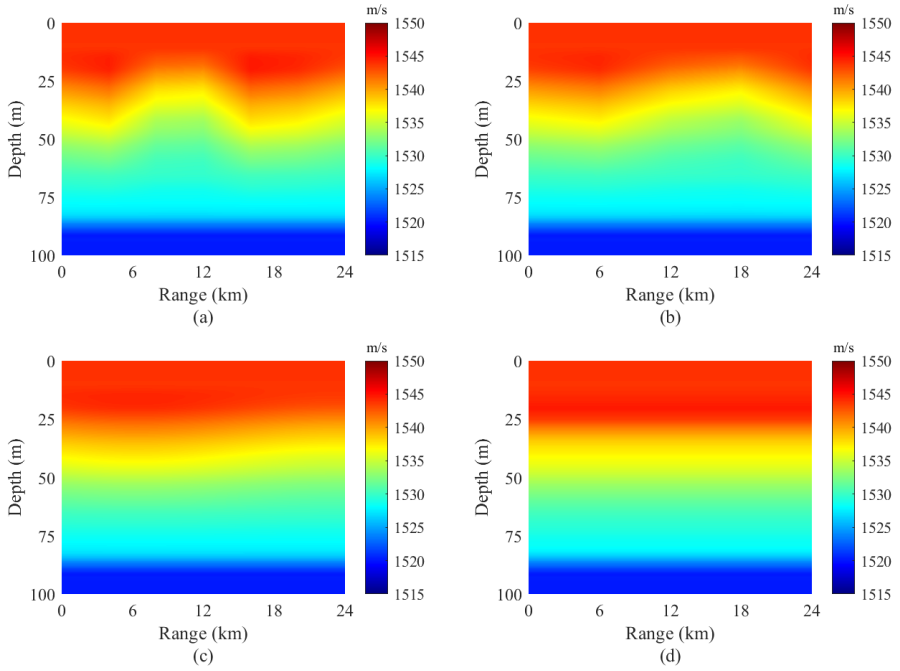

Fig. 8. Reconstructed equivalent sound speed profiles in experiment.

(a) Linear equivalent SSP ($\Delta r = 4$ km); (b) Linear equivalent SSP ($\Delta r = 6$ km);

(c) Periodic equivalent SSP; (d) Range-independent SSP.

5 Conclusion

The temporal variations of the SSPs are represented using basis functions such as EOF, where vertical fluctuations are captured through the estimation of corresponding coefficients. To account for the range dependence of the environmental SSP associated with internal waves, two range-dependent equivalent SSP models are investigated: (1) a piecewise linear equivalent SSP model that approximates variations by using multiple segments over distance, and (2) a continuous periodic equivalent SSP model that represents range dependence based on the dominant tidal constituents of the environment. The segmentation interval in the linear equivalent SSP model and the wavelength search range in the periodic equivalent SSP model are determined by environmental prior knowledge. Both range-dependent MFP algorithms—based on the linear and periodic equivalent SSP models—outperform the conventional range-independent MFP method, which neglects spatial variability in the environmental SSP. Numerical simulations and experimental results from the South China Sea confirm the feasibility and effectiveness of incorporating range-dependent equivalent SSP models to improve MFP-based source localization in shallow-water internal wave environments.

References

[1] H. P. Bucker, “Use of calculated sound fields and matched-field detection to locate sound sources in shallow water,” *J. Acoust. Soc. Am.*, vol. 59, no. 2, pp. 368–373, 1976, doi: 10.1121/1.380872.

[2] Y.F. Li, R. M. Guo, and H. F. Zhao, ”Sparse reconstruction of acoustic interference fringes in shallow water and internal wave environment,” *Acta Physica Sinica*, vol. 72, no. 7, pp. 074301, 2023, doi: 10.7498/aps.72.20221932

[3] Schmidr H, Baggeroer A B, Kuperman W A, et al. Environmentally tolerant beamforming for high-resolution matched field processing: deterministic

mismatch[J]. Journal of the Acoustical Society of America, 1990, 88(4): 1851–1862.

[4] Richardson A M, Nolte L W. A posteriori probability source localization in an uncertain sound speed, deep ocean environment[J]. Journal of the Acoustical Society of America, 1991, 89(5): 2280–2284.

[5] Shorey J A, Nolte L W, Krolik J L. Computationally efficient Monte Carlo estimation algorithms for matched field processing in uncertain ocean environments[J]. Journal of Computational Acoustics, 1994, 2(3): 285–314.

[6] Seong W, Byun S H. Robust matched field-processing algorithm based on feature extraction[J]. IEEE Journal of Oceanic Engineering, 2002, 27(3): 642–652.

[7] Michael D. Collins, W. A. Kuperman. Focalization: Environmental focusing and source localization[J]. *J. Acoust. Soc. Am.*, 1991; 90: 1410-1422.

[8] Ralph N. Baer, Michael D. Collins. Source localization in the presence of internal waves[J]. *J. Acoust. Soc. Am.*, 2005; 118: 3117-3121.

[9] Rachel M. Hamson, Richard M. Heitmeyer. Environmental and system effects on source localization in shallow water by the matched-field processing of a vertical array[J]. *J. Acoust. Soc. Am.*, 1989; 86: 1950-1959

[10] Lester R. LeBlanc, Forster H. Middleton. An underwater acoustic sound velocity data model[J]. *J. Acoust. Soc. Am.*, 1980; 67: 2055-2062.

[11] Cristiano Soares, Martin Siderius, and Sergio M. Jesus. Source localization in a time-varying ocean waveguide[J]. *J. Acoust. Soc. Am.*, 2002; 112: 1879-1889.

[12] Peter Gerstoft, Donald F. Gingras. Parameter estimation using multifrequency range-dependent acoustic data in shallow water[J]. *J. Acoust. Soc. Am.*, 1996; 99: 2839-2850.

[13] A.G. Sazontov, I.P. Smirnov. Source Localization in an Acoustic Waveguide with Inaccurately Known Parameters Using Matched Processing in the Mode Space[J]. *Acoust. Phys*., 2019; 65: 450-459.

[14] T. C. Yang and K. Yoo, "Internal wave spectrum in shallow water: measurement and comparison with the Garrett-Munk model," *IEEE Journal of Oceanic Engineering*, vol. 24, no. 3, pp. 333-345, 1999, doi: 10.1109/48.775295.

[15] W. Song, T. Hu, S. M. Guo, L. Ma, and L. L. Lu, "A methodology to achieve the basis for the expansion of the sound speed profile," *Acta Acustica*, vol. 39, no. 1, pp. 11–18, 2014, doi: 10.15949/j.cnki.0371-0025.2014.01.001

[16] K. Qu, S. C. Piao, and F. Q. Zhu, "A noval method of constructing shallow water sound speed profile based on dynamic characteristic of internal tides," *Acta Phys. Sin.*, vol. 68, no. 12, pp. 124302, 2019, doi: 10.7498/aps.68.20181867.

[17] Harry A and DeFerrari, "Effects of horizontally varying internal wavefields on multipath interference for propagation through the deep sound channel," *J. Acoust. Soc. Am.*, vol. 56, no. 1, pp. 40–46, 1974.

[18] Zhen Wang, Tao Hu, W. B. Wang, S. M. Guo, and Li Ma, "Characteristics of coastal internal waves and acoustic-energy fluctuations in the South China Sea in summer," *ACTA ACUSTICA*, vol. 49, no. 1, pp. 67-77, 2024, doi: 10.12395/0371-0025.2023147.

[19] G. H. Ji, and Z. L. Li, "The coherence-time of matched-field processing with the presence of the linear internal waves in the South China Sea," *Acta Acustica*, vol. 36, no.1, pp. 1-7, 2011, doi: 10.15949/j.cnki.0371-0025.2011.01.001.

[20] P. Qian, W. M. Gan, H. Q. Niu, G. H. Ji, Z. L. Li, and G. J. Li, "A feature-compressed multi-task learning U-Net for shallow-water source localization in the

presence of internal waves," *Applied Acoustics*, vol. 211, no.4, pp. 109530, 2023, doi: 10.1016/j.apacoust.2023.109530.